Effects of Salts on the Micellization and Gelation of a Triblock Copolymer Studied by Rheology and Light Scattering

Erling B. Jørgensen* and Søren Hvidt

Department of Chemistry, Roskilde University, DK-4000 Roskilde, Denmark

Wyn Brown and Karin Schillén

Department of Physical Chemistry, University of Uppsala, S-751 21 Uppsala, Sweden

Received November 5, 1996; Revised Manuscript Received February 13, 1997[⊗]

ABSTRACT: The phase behavior and aggregation properties of a triblock copolymer of ethylene oxide (EO) and propylene oxide (PO), with a measured composition $(EO)_{29}(PO)_{40}(EO)_{29}$, in aqueous solutions containing salt, have been examined using dynamic light scattering, rheological techniques, and sedimentation and viscosity measurements. The copolymer is dissolved as a unimer at low temperatures and forms spherical micelles with increasing temperature. At higher temperatures, a sphere-to-rod transition is seen for the micelles. Two types of gel are formed at higher concentrations of the copolymer. With different inorganic salts, the micellization and gelation properties of the copolymer follow the same type of transitions as the salt-free system, but all transition temperatures are shifted. The spherical micelles thus transform into rod-like micelles at around 38 °C in 1 M KF, which is approximately 36 deg below the transition temperature in the salt-free system. Rod lengths in 1 M KF are between 1000 and 1800 Å, at 40 °C. The higher-temperature gel phase is seen at all concentrations down to 0.5 −1 wt %. The elasticity of this gel is due to hindered rotation of rods. Its relaxation time decreases with increasing concentration, indicating that the gel relaxes due to a partial breakdown or dissolution of the rods at the cross points. The strain dependence of this gel suggests that ordered structures of rods are formed at concentrations above 27 wt %.

I. Introduction

Block copolymers of ethylene oxide (EO) and propylene oxide (PO) are nonionic surfactants with a large number of applications.[1] Symmetrical triblock copolymers, with structure $(EO)_m(PO)_n(EO)_m$, where m and n denote the number of EO and PO monomers per block, are commercially available with a broad range of block sizes. The complex solubility and aggregation behavior of these copolymers in aqueous solution have received intensive attention in the literature, as for example, discussed in a number of recent reviews.[2−4] At low temperatures some of these copolymers are soluble in aqueous solution as unimers, but form micelles at higher temperatures.[5−9] Micelle formation is driven by the hydrophobic PPO block,[10−12] with a core consisting of PPO blocks and a corona of PEO blocks.[13] The copolymer micellizes by a closed association mechanism, where the unimers and micelles exist in equilibrium.[14] The lifetime of a unimer within a micelle has been estimated to be approximately 1 μs at 20 °C.[15]

Micelles grow in molecular weight with temperature but not with concentration.[16,17] For some copolymers the micelles eventually reach a maximum diameter of the spherical micellar core, determined by an entropically unfavorable stretching of the PPO block.[8,18,19] At even higher temperatures rod-like micelles are formed, which, for the copolymer P-85 with a nominal composition $(EO)_{27}(PO)_{39}(EO)_{27}$, have an estimated length of approximately 1050 Å at 75 °C.[20] The micellar length increases with temperature nearly up to the cloud point temperature, where the rods aggregate.

At high concentrations of some triblock copolymers the spherical micelles close-pack in a cubic (bcc) structure,[17,21] and the system exhibits gel-like behavior.[8,11,22,23] At higher temperatures some copolymers form another gel-state,[11,22] which at high concentrations consists of rod-like micelles packed in a hexagonal structure.[18]

The effect of salt on the clouding temperature and micellization behavior of EO-containing nonionic surfactants is primarily controlled by the polarizability of the ions.[24−26] The same effect is seen for the clouding temperature of PEO.[27,28] These effects are mainly ascribed to the change in water structure due to interactions between the inorganic salt and water.[28] Structure makers are salts like KCl and KF, which lead to an increase in the self-hydration of water through hydrogen-bonding, and therefore a reduction in polymer solubility. Structure breakers are salts like KI and KSCN, which reduce self-hydration and thereby increase the hydration of the polymer. The hydration is also increased by hydrogen-bonding to the ether oxygens in the polymer. Binana-Limbelé and co-workers[25] have determined the aggregation number, N, of micelles as a function of temperature with different inorganic salts. The N values were independent of salt type when compared at similar temperatures below the respective cloud temperatures, T_{cp}. Bahadur and co-workers[26] have also observed constant N values and constant intrinsic viscosities at a fixed temperature difference $(T_{cp} - T)$.

In this study we have investigated the influence of inorganic salts on a triblock copolymer designated P-85 with the nominal composition $(EO)_{27}(PO)_{39}(EO)_{27}$. The effects on micellization, gelation, and clouding have been studied. The effect on the sphere-to-rod transition temperature was studied by light scattering, viscometry, and sedimentation. Dynamic light scattering was used to estimate the micellar rod length. The gelation of the micellar rods and the properties of the gel resulting at higher concentrations were analyzed with respect to concentration and temperature, and deformation was

* Corresponding author's present address: Department of Solid State Physics, Risø National Laboratory, DK-4000 Roskilde Denmark. E-mail: bonne.joergensen@risoe.dk.

[⊗] Abstract published in *Advance ACS Abstracts,* April 1, 1997.

S0024-9297(96)01632-4 CCC: $14.00

analyzed by viscoelastic measurements. The deformation dependence of the gel state formed by spherical micelles at high concentration was also studied by viscoelastic measurements.

II. Experimental Section

A. Materials. The nonionic surfactant P-85, a symmetric triblock copolymer was obtained from Serva AG in Heidelberg, Germany. The copolymer was purified by extraction of the more hydrophobic impurities with *n*-hexane. About 100 g of P-85 was extracted five times with 225 mL of *n*-hexane at 39 °C in a thermostat with gentle shaking. The remaining polymer was dried in vacuum. This is a modification of a published method.[29] The unpurified P-85 sample contained some more hydrophobic components, which interfere with light scattering experiments at low temperature.[11] This impurity was largely removed during the extraction.

The purified P-85 was characterized by use of ^{1}H and ^{13}C NMR as described for a similar triblock copolymer.[11] The results show that P-85 contains 47.6 wt % PO and has a number average composition of $EO_{29}PO_{40}EO_{29}$, which corresponds to a molecular weight of 4870.

The inorganic salts KF, KCl, and KSCN were all analytical grade from Merck.

Solutions of P-85 in distilled water and salt solutions were prepared gravimetrically and allowed to dissolve and mix at 5 °C with gentle shaking overnight. Concentrations of copolymer reported here are all given as weight−weight percent (wt %, grams of polymer per 100 g of solution). Solutions containing salts were prepared by addition of copolymer to the salt solution in water (0.5 and 1.0 M). This means that the salt concentration in the copolymer solutions is slightly less than the stated 0.5 and 1.0 M. However, the ratio of salt to water is kept constant.

The samples for sedimentation and light scattering measurements were filtered at 5 °C through 0.22 μm Millipore (Durapore) filters into 10 mL cylindrical ampules and flame-sealed under a N_2 atmosphere.

B. Rheological Techniques. Viscoelastic measurements were performed on a Bohlin VOR rheometer (Lund, Sweden) using a stainless steel couette geometry (inner diameter 14 mm; outer diameter 15.4 mm; height 21 mm). The narrow gap ensures a virtually constant shear deformation through the sample. The outer cylinder is surrounded by a water bath which is connected to a thermostat bath. In heating and cooling measurements, the temperature was typically varied in steps of 0.5 deg with 2 min equilibration time at each temperature. Cold copolymer solutions were transferred to the instrument and carefully overlaid with a low-viscosity silicone oil to minimize water evaporation. The instrument measures the temperature in the bath next to the outer cylinder. A temperature correction calibration curve was determined by use of a Grant microthermistor, which was placed in the solution between the inner and outer cylinder in a series of calibration measurements. In the temperature-sweep and strain-sweep measurements, the VOR instrument was used in the oscillatory mode, where the outer cylinder performs oscillations at a given frequency, here chosen to be 0.15 Hz. The storage and loss shear moduli, G' and G'', are obtained from the time dependence of the stress, σ, by use of the definition[30]

$$\sigma = \gamma_0(G' \sin \omega t + G'' \cos \omega t) \tag{1}$$

where γ_0 is the strain amplitude and ω is the radian frequency. The strain amplitude can be varied between 0.001 and 0.2 on the instrument. It was ensured that the temperature-sweep and frequency-sweep measurements were obtained in the linear viscoelastic region, where G' and G'' are independent of the strain amplitude. The frequency of oscillation can be varied between 0.001 and 20 Hz. Stress relaxation was performed as a supplement to frequency sweeps in order to determine relaxation times. The sample is rapidly (<0.1 s) deformed to a constant shear strain in a stress relaxation measurement, and the stress required to maintain this deformation is measured as a function of time.

A simple falling-ball-type viscometer, described in the earlier paper,[11] was used as an independent way to determine gelation and degelation temperatures.

Specific and intrinsic viscosities were determined by use of an Ubbelohde capillary viscometer.

C. Dynamic Light Scattering Measurements. The light scattering measurements were made using a Coherent Innova Ar ion laser operating at 488 nm. A Glan-Thompson polarizer (extinction 10^{-6}) defined the vertical polarization. The detector optics employed a 4 μm diameter monomodal fiber coupled to an ITT FW 130 photomultiplier, the output of which was digitized by an ALV-PM-PD amplifier-discriminator. The signal analyzer was an ALV-5000 digital multiple-τ correlator. The DLS data were analyzed by nonlinear regression procedures. The models used in the fitting procedure are expressed with respect to the normalized electric field correlation function, $g^{(1)}(t)$, which can be written as the Laplace transform of the distribution of relaxation times, τ:

$$g^{(1)}(t) = \int_{-\infty}^{\infty} \tau A(\tau) \exp(-t/\tau)\, \mathrm{d} \ln \tau \tag{2}$$

The relaxation time distributions are given in the form of $\tau A(\tau)$ vs log τ. $\tau A(\tau)$ was obtained from inverse Laplace transformation of the intensity correlation functions using the REPES-constrained regularization program.[6,31] For the measurements on rod-like micelles, supplementary data analyses were made using a double-exponential function, also from the analysis package GENDIST.[20]

The length of a micellar rod can be estimated by DLS if the micelles are sufficiently asymmetric such that the rotational diffusion coefficient can be measured. Pecora[32] has shown that for optically isotropic rods in solution the normalized electric field correlation function, $g^{(1)}(t)$, may be expanded to give a weighted sum of two (or more) exponential decays. The first term is the purely translational part, and the second term is related to the rotational diffusion about the center of the rod:

$$g^{(1)}(t) = S(q,t) = S_0(qL) \exp(-q^2 D t) + S_1(qL) \exp(-(q^2 D + 6\theta)t) + \ldots \tag{3}$$

D in eq 3 is the translational diffusion coefficient, L is the rod length, θ is the rotational diffusion coefficient, and q is the scattering vector. At $qL > 3$, the amplitude, $S_1(qL)$, of the second decay rate (Γ_f) becomes sufficiently large that it is possible to estimate the rotational diffusion coefficient (θ).[33] Since the sum of the terms higher than those shown in eq 3 is negligible for $qL < 8$, then

$$6\theta = \Gamma_f - q^2 D \tag{4}$$

and the quantity θ can be obtained directly in the limit $q \rightarrow 0$.

From Broersma's relationships for rigid noninteracting rods of diameter d at infinite dilution, with $L/d > 5$, it is possible to estimate the length, from θ and D.[34−37]

$$\theta = \frac{3kT}{\pi \eta_0 L^3}(\delta - \zeta) \tag{5}$$

where $\delta = \ln(2L/d)$, and $\zeta = 1.45 - 7.5(1/\delta - 0.27)^2$

$$D = \frac{kT}{3\pi \eta_0 L}(\delta - 0.5(\gamma_{\parallel} + \gamma_{\perp})) \tag{6}$$

where $\gamma_{\parallel} = 1.27 - 7.4(1/\delta - 0.34)^2$ and $\gamma_{\perp} = 0.19 - 4.2(1/\delta - 0.39)^2$ and η_0 is the solvent viscosity.

It was possible to obtain an alternative estimate of the rod length by fitting a constructed intensity autocorrelation function based on the normalized electric field correlation function for a rodlike micelle to the experimental data. The detailed

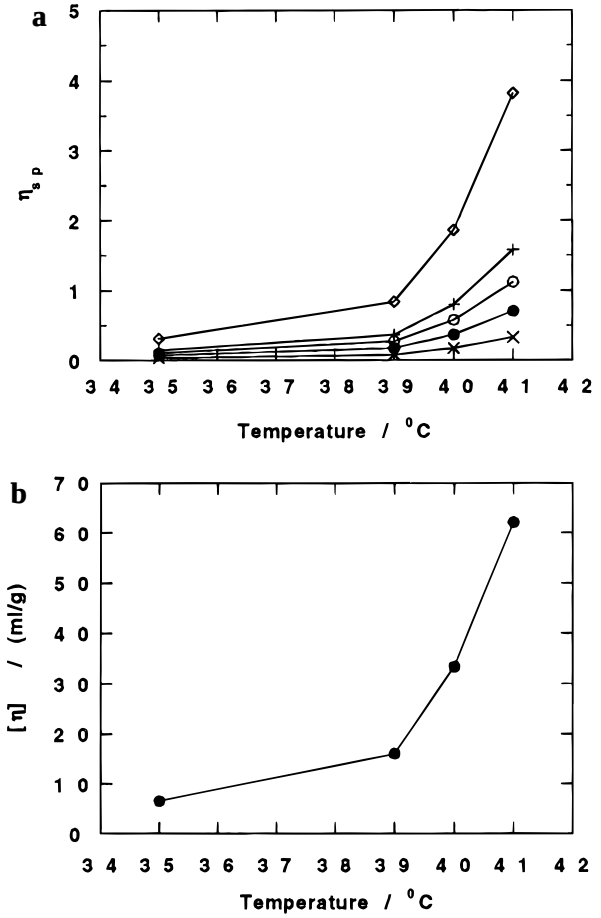

Figure 1. (a) Specific viscosity against temperature for five concentrations of P-85 in 1 M KF: 0.5 wt % (×); 1.0 wt % (●); 1.5 wt % (○); 2.0 wt % (+); and 4.0 wt % (◇). (b) The corresponding intrinsic viscosity against temperature.

description for this procedure has been given by Schillén et al.[20] The fitting program GENROD is also incorporated in GENDIST.

D. Other Techniques. Sedimentation measurements were made using an MSE analytical ultracentrifuge (Centriscan 75) equipped with schlieren optics. Sedimentation coefficients were determined at a rotation rate of 54 000 rpm.

Cloud points were determined by visual inspection of solutions in sealed thin-walled glass tubes with a diameter of 5 mm. The tubes were placed in a thermostat, and temperatures were increased or decreased in steps of 0.5 or 1 deg with 5 min equilibration time. The temperatures of initial clouding and complete declouding were determined visually.

III. Results and Discussion

A. Sphere-to-Rod Transition. The expected sphere-to-rod micellar transition was examined by a number of different experimental techniques, i.e. viscosity and sedimentation measurements and light scattering measurements, which are sensitive to the length and asymmetry of the micelles. The temperature dependence of the viscosity for five concentrations of P-85 in 1 M KF is presented in Figure 1a. The specific viscosity increases strongly at around 40 °C, indicating a transition in shape of the micelles. Figure 1b shows the corresponding intrinsic viscosity results which confirm the transition in this temperature range. The intrinsic viscosity increases by a factor of 10 over a narrow temperature range of 6 deg. This reflects a strong increase of the specific hydrodynamic volume. For comparison, the intrinsic viscosity only changes from 13 to 6 mL/g during micellization at lower temperatures.

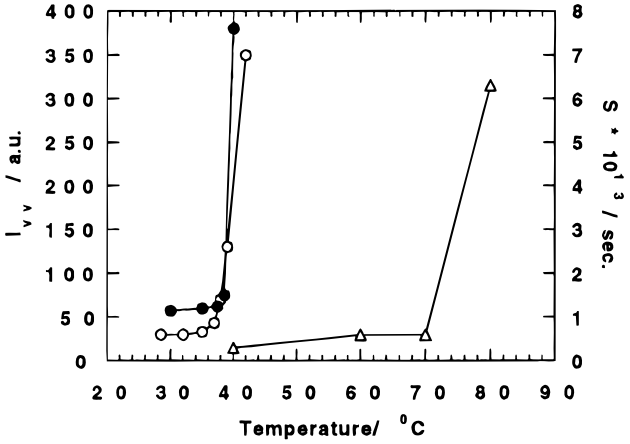

Figure 2. Polarized scattered intensity at Θ = 90° as a function of temperature for solutions of 0.1 wt % P-85 in 1 M KF (○) and in water[18] (△). Sedimentation coefficient at infinite dilution of P-85 micelles in 1 M KF (●), as a function of temperature. The coefficients are normalized with respect to solvent viscosity and density of water at 25 °C for comparison.

The observed large increase near 40 °C corresponds to the transition from spherical to rod-like micelles.

The formation of rod-like micelles also increases the micellar mass, which can be monitored by sedimentation measurements. Four samples with concentrations of P-85 between 0.4 and 1.3 wt % in 1 M KF were measured. Figure 2 shows the sedimentation coefficient extrapolated to infinite dilution plotted against temperature. The increase is clearly seen around 40 °C, corresponding to a pronounced growth in micellar mass. The increase in micellar mass is also seen in static light scattering. The polarized scattering intensity measured at an angle of 90° for a solution of 0.1 wt % P-85 in 1 M KF is presented in Figure 2 as a function of temperature. The intensity increase corresponds to a growth in the apparent micellar mass of the order of 8 times going from 32 to 42 °C. For comparison, similar data obtained on the salt-free system[20] are included. It is seen that 1 M KF shifts the transition temperature by approximately 36 deg with respect to the salt-free solution.

For a 0.3 wt % P-85 solution in 1 M KF, free unimers of P-85 exist in a nonaggregated state at low temperatures. At around 10 °C spherical micelles start to form. This transition was detected by dynamic light scattering measurements (not shown). The dynamic light scattering data on the 0.3 wt % solution in 1 M KF at higher temperatures from 25 to 43.2 °C are illustrated in Figure 3a by the relaxation time distributions obtained by regularized inverse Laplace transformation (RILT) of the data. The distributions have been corrected for changes in viscosity and temperature. At 25 °C the relaxation time distribution is single modal, corresponding to spherical micelles. A weak increase in micellar size is observed up to 36 °C (corresponds to a peak shift to slower relaxation times). At 37.4 °C, significant micellar growth is clearly detected. In the temperature range where the other techniques indicate the transition, the relaxation time distribution thus changes from a single mode to bimodal, as expected for asymmetric micellar rods. Figure 3b shows an enlarged version of the distribution at 39.3 °C. This clearly shows the presence of a low amplitude fast peak that corresponds to a combination of rotational diffusion relaxation and translational diffusion according to eq 3 (see below). The dominant slow mode corresponds to the translational

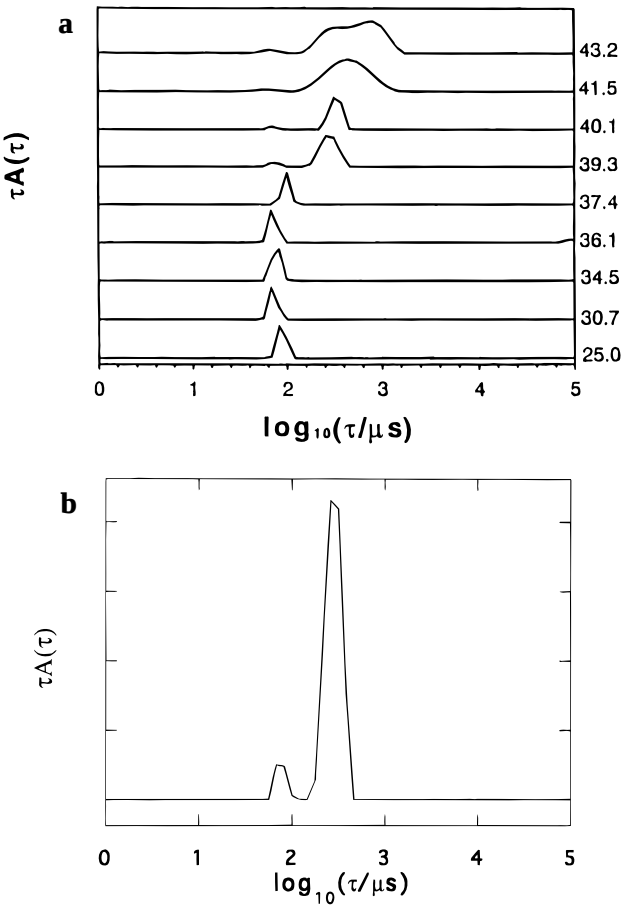

Figure 3. (a) Relaxation time distributions obtained by regularized inverse Laplace transformation of dynamic light scattering data, $\tau A(\tau)$ versus log τ/μs, for 0.025 wt % P-85 in 1 M KF at temperatures between 25 and 43.2 °C. The temperatures in °C are indicated on the right axis. Measurements are performed at an angle of 90°. (b) An enlarged version of the distribution at 39.3 °C.

diffusion of rods. This mode changes rapidly with temperature to even longer relaxation times. At 41.5 °C the distribution starts to broaden and eventually the slow translational peak splits into two broad peaks at 43.2 °C. The slower motion observed at 43.2 °C may be due to intermicellar aggregation, which makes the sample slightly opaque at higher temperatures and concentration.

Eight solutions of P-85 in 1 M KF with concentrations between 0.025 and 5.0 wt % were measured by DLS in order to determine the hydrodynamic radii of the unimers and micelles. It was established that the relaxation rates, for the unimers and both micellar types, are q^2-dependent, passing through the origin. This shows that the observed modes are diffusive. Extrapolations of diffusion coefficients to infinite dilution (D_0) are used in the Stokes−Einstein relationship, $R_H = kT/6\pi\eta_o D_o$. R_H of the free unimers is 19 Å, which is approximately equal to the unimer dimension in the salt-free system (18 Å).[38] The radius of the micelles, on the other hand, increases from around 80 to 92 Å between 15 and 34 °C. These values are somewhat larger than the 75 Å previously found in the salt-free system.[39] Above the sphere-to-rod transition temperature, R_H of the micelles increases from almost 400 Å to more than 500 Å. These values were obtained from measurements on low concentration solutions in order to minimize interference from micellar aggregation.

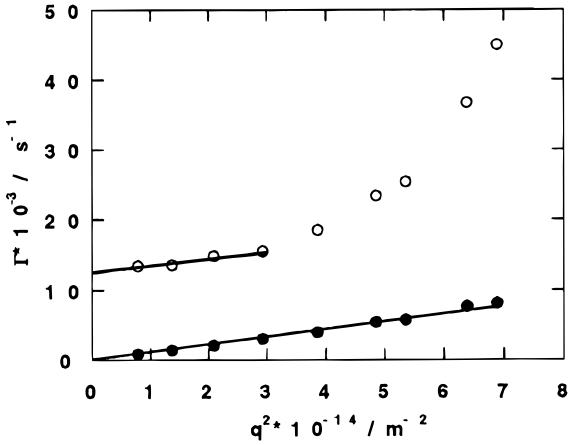

Figure 4. Two relaxation rates for 0.025 wt % P-85 in 1 M KF at 40 °C, at scattering angles between 30 and 100° are plotted as a function of the squared scattering vector. The slower (●) is the translational diffusion mode, and the fast (○) corresponds to the second term in eq 3.

Similar DLS measurements were made for P-85 in 0.5 M KF. R_H for the unimers is again 19 Å, and micellar formation starts around 15 °C. These spherical micelles are fairly constant in size (R_H = 79 Å) in the temperature range up to the sphere-to-rod transition, which occurs at 54 °C.

At temperatures above the sphere-to-rod transition, the relaxation time distributions become bimodal (Figure 3). In Figure 4, the two relaxation rates, obtained from RILT of the dynamic light scattering data, are plotted against the square of the scattering vector for 0.025 wt % P-85 in 1 M KF at 40 °C. For the slow mode, which corresponds to the translational motion of the micellar rods, the relaxation rate, Γ_s, is linear in q^2 and the slope equals the translational diffusion coefficient. The fast mode is a combination of rotational and translational motions of the rods.[20] The rotational diffusion coefficient, θ, is obtained by extrapolating the relaxation rate, Γ_f, to vanishing scattering vector q = 0, since $(\Gamma_f)_{q=0} = 6\theta$ (see eq 4). DLS measurements were performed at two additional concentrations at temperatures between 40 and 45 °C, where the micelles are rodlike and the relaxation time distributions were bimodal, as in Figure 3. In order to check the relaxation time distributions the data were also analyzed by the William−Watts double-exponential method,[20] and both methods gave results in good agreement. The translational and the rotational diffusion coefficients for the different concentrations of P-85 in 1 M KF at 40 °C are given in Table 1a.

B. Length of Rods. The rotational and translational diffusion coefficients can be used to obtain independent estimates of the length of the micellar rods (see eqs 5 and 6). Two approaches were applied to estimate the rod length of the micelle. In the first approach, the length (L_1) is directly interpolated from eq 5 using the rotational diffusion coefficient obtained from the fast relaxation rate at $q = 0$ in Figure 4. The diameter, d, was set to twice the hydrodynamic radius of the spherical micelle (R_H = 92 Å), just before transition. Linse[19] has predicted that the radial extension should be reduced abruptly by ca. 10% at the sphere-to-rod transition. This means that the used value for d might be overestimated and the length therefore underestimated.

In the second approach (giving L_2), the DLS data are fitted using the rod model.[20] To estimate the rod length,

Table 1. Translational and Rotational Diffusion Coefficients and Rod Lengths for P-85 in 1 M KF

a. Temperature: 40 °C

c (wt %)	$10^{12}D$ (m^2/s)	$10^{-3}\theta^a$ (s^{-1})	$L_1{}^b$ (Å)	$L_2{}^c$ (Å)	$10^{12}D_{ROD}{}^d$ (m^2/s)
0.005	17.5	2.75	1470	500	17.9
0.025	11.3	1.95	1690	1000	11.7
0.100	9.05	0.83	2060	1800	8.77

b. Concentration: 0.005 wt %

T (°C)	$10^{12}D$ (m^2/s)	$10^{-3}\theta^a$ (s^{-1})	$L_1{}^b$ (Å)	$L_2{}^c$ (Å)	$10^{12}D_{ROD}{}^d$ (m^2/s)
40	17.5	2.75	1470	500	17.9
42	13.3	1.76	1860	850	13.3
45	12.5	1.68	1880	1100	12.6

c. Concentration: 0.025 wt %

T (°C)	$10^{12}D$ (m^2/s)	$10^{-3}\theta^a$ (s^{-1})	$L_1{}^b$ (Å)	$L_2{}^c$ (Å)	$10^{12}D_{ROD}{}^d$ (m^2/s)
40	11.3	1.95	1690	1000	11.7
42	8.92	1.75	2380	2200	8.19
45	8.41	0.62	2830	3050	7.18

[a] Equation 3. [b] Equation 4. [c] Fitting method. [d] Equation 5 with L_2.

L_2, a constructed intensity autocorrelation function based on the normalized electric field correlation function was fitted to the experimental data. Again d was set to twice the R_H. As a check of the fitted length, L_2, the corresponding theoretical translational diffusion coefficient, D_{ROD}, was calculated from eq 6, for comparison with the measured, D. The estimates of the micellar rod length using a rigid-rod model may not give exact lengths since the micellar rods are presumably not completely inflexible. To make a good estimate of the rod length, it is necessary to measure very dilute solutions in order to avoid or minimize frictional interactions between the micelles, but still at concentrations above the critical micelle concentration (cmc). The two estimates of the rod length and a theoretical value for D, calculated from the fitted rod length, are also given in Table 1a.

The estimated length at 40 °C shown in Table 1a clearly indicates a concentration dependence, although the measurements on the very dilute solution and at the highest concentration contain greater uncertainty. The very dilute solution at 40 °C may still contain spherical micelles in an amount that could influence the determination of the fast relaxation time. It has been concluded in earlier investigations,[16,17] on the other hand, that the micelles do not grow with increasing concentration but that they grow with temperature. The present results are not conclusive concerning possible growth with concentration since interparticle interaction leading to translational/rotational coupling will become increasingly important. It is also not possible from these few concentrations to determine a critical concentration for interaction of the rods, but measurements on the salt-free system[20] gave an upper limit of about 0.05 wt % for the rods with an estimated length of ca. 1050 Å. The solution of 0.1 wt % P-85 in 1 M KF is therefore most likely well above the concentration range where the rods are noninteracting. Interaction between rods will decrease the diffusion coefficient and thereby overestimate the length. The fitting method shows the strongest dependence on the diameter of the rods. Underestimation of the length will therefore be strongest for L_2. An independent check of L_2 by comparison of the measured D value and the calculated D_{ROD} shows good agreement. The differences in the estimated lengths, L_1 and L_2, is probably due to the uncertain d value, which has different weightings in the estimates from θ and D, respectively.

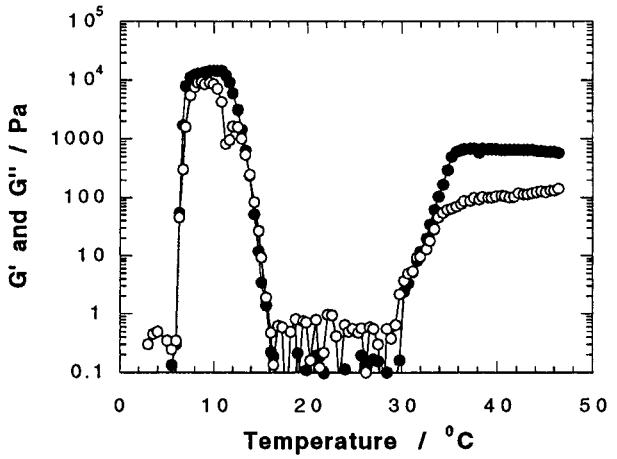

Figure 5. Viscoelastic properties of 28.5 wt % P-85 in 1 M KF as a function of temperature at 0.15 Hz. (●) G' and (○) G'' are the storage and loss moduli, respectively.

Parts b and c of Table 1 show a temperature dependence of the micellar rod length for 0.005 and 0.025 wt %, respectively. Due to the increasing length, the critical concentration for interactions between the rods decreases with temperature. The estimates for the higher temperatures in Table 1c may therefore be too large. The temperature and concentration ranges where these estimations are reliable are therefore limited for this salt−micelle system. In summary, the estimated rod length at 40 °C lies between 1000 and 1700 Å and micellar growth occurs with temperature up to 2000 Å. These dimensions give L/d ratios from around 6 to 11, which means short and bulky micelles.

C. Viscoelastic Results. Rod-like micelles at higher concentrations induce gel-like behavior. Due to the hindered rotation of the rods the relaxation times will increase to the order of seconds, when the concentration exceeds the critical number density concentration ($c^* = 1/L^3$).[40] Viscoelastic measurements were performed, both to detect the gel formation and its temperature limits and to analyze the properties of the gel. Figure 5 shows the oscillatory shear results for 28.5 wt % P-85 in 1 M KF as a function of temperature measured at a frequency of 0.15 Hz. At low temperatures a viscoelastic liquid is observed, since $G'' > G'$. Around 6 °C, G' increases abruptly and reaches larger values than G''. The elastic storage modulus reaches a maximum around 11 °C, where the loss modulus has a minimum value. This shows that the viscous solution changes to a gel-like state with increasing temperature. At temperatures above 13 °C both G' and G'' decrease rapidly, and at temperatures between 16 and 30 °C a new viscoelastic liquid is formed, since G'' exceeds G'. A second gel structure is formed at temperatures above 33 °C, and it exists in the temperature range where the micelles are rod-like. The elastic modulus of this gel is more than 1 order of magnitude lower than the former. The low-temperature gel will be referred to as the "hard gel", and the high-temperature gel, as the "soft gel". This phase profile, showing two gel states is similar to that earlier observed in the salt-free system[5,41] and the P-94 system.[11] The temperatures for all transitions in 1 M KF are shifted to lower temperatures when compared to the salt-free P-85 system. SANS measurements[21] on

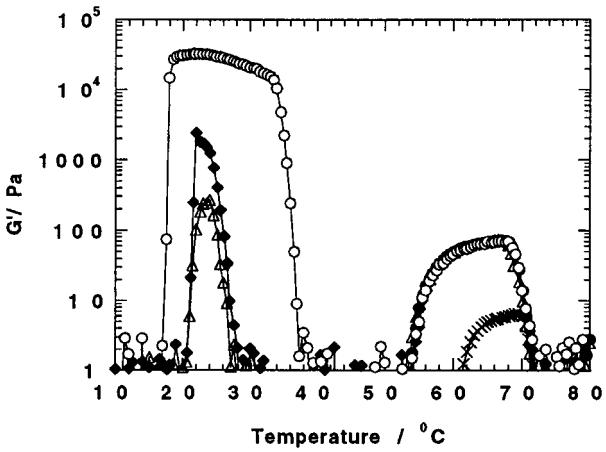

Figure 6. G' for P-85 in 1 M KCl as a function of temperature at 0.15 Hz for solutions with concentrations in wt %: (×) 5.0; (●) 23.2; (△) 23.4; (◆) 23.8; (○) 25.0.

the salt-free P-85 systems have shown that the hard gel consists of close-packed spherical micelles in a cubic (bcc) structure. At high concentrations the soft gel is considered to be an ordered structure of rod-shaped micelles in a hexagonal structure.[20,21] At the highest temperatures shown in Figure 5, the gel state exists above the cloud temperature, which for this concentration is around 40 °C. This behavior contrasts with that in the salt-free P-85 system[26] and the P-94 system,[11] where degelation occurs at the clouding temperature.

The temperature-dependent viscoelastic properties were measured at different concentrations of P-85 in 1 M KF, 0.5 M KF, 1 M KCl, and 1 M KSCN to study the salt effects on transition temperatures and critical gelation concentrations. Due to the special aggregation/clouding behavior in KF, which complicates the picture, the following discussions will concentrate on the KCl system.

A concentration dependence of the temperature-dependent viscoelastic properties is seen for both the hard and the soft gels in Figure 6, where G' for five different concentrations of P-85 in 1 M KCl is plotted as a function of temperature. The concentration dependences of the two gels are different. The hard gel is not formed at concentrations up to 23.3 wt %, whereas the solutions above this concentration form a gel with $G' > G''$ and a maximum G' value at about 23 °C. The critical gelation concentration (cgc) is 23.4 ± 0.1 wt %. It is seen that a small increase in concentration affects both the storage modulus, which increases, and the width of the temperature region for this gel. The gel is stabilized at both higher and lower temperatures when the concentration is increased. The concentration dependence of the soft gel is much smaller. The gel is formed at all concentrations down to 0.5 wt %, and the effect of decreasing concentrations is to decrease the storage modulus and to reduce the gel temperature region. For this gel, variations in concentration only affect the onset temperature. The degelation temperatures are almost constant.

In the P-85/1 M KCl system it is seen that the various temperature transitions are shifted downward in temperature compared to the salt-free system, but not as effectively as in 1 M KF (Figure 5).

The effect of KSCN addition on the temperature dependence of the phase behavior of P-85 is opposite to the two other investigated salts. The transitions are shifted upward in temperature compared to the salt-free system. The directions of the effects of these three salts are in agreement with other studies of a number of polymers with respect to their cloud points.[24−27]

Table 2. Transition Temperatures (°C) for P-85 in Pure Aqueous and Salt Containing Solutions[a]

solvents	cloud point[b]	rods[c]	soft gel[d]	hard gel[e]
pure H_2O	87	74	82	39
1 M KF	50 (37)	38 (36)	47 (35)	11 (28)
0.5 M KF	68 (19)	54 (20)	63 (19)	24 (15)
1 M KCl	72 (15)		63 (19)	23 (16)
1 M KSCN	97 (−10)		91 (−9)	42 (−3)

[a] The numbers in parentheses are ΔT ($T_{H_2O} - T_{salt}$). [b] Cloud point temperatures for 1 wt % solutions. [c] Onset temperatures of formation of rods for 0.1 wt % solutions. [d] Onset temperatures for formation of soft gels for 1 wt % solutions. [e] Onset temperatures for formation of hard gels for solutions at the critical gelation concentration.

A simple falling-ball-type viscometer was used as a supplement and as an independent way to determine gelation and degelation temperatures. This method also detects the hard and the soft gels, and the observed transition temperatures for the hard gel are in agreement with those obtained with the rheometer. For the soft gel the onset temperature is typically 5 °C above the rheometer temperature, which may be due to the fact that the falling-ball-type viscometer determines a yield stress. The yield stress is expected to be very low near the gel point for the soft gel due to its low G' value.

D. Comparison of Salt Effects. The observed temperature effects of the salts on P-85 solutions are summarized in Table 2 with respect to four characteristic transitions: cloud points at 1 wt %; sphere-to-rod transition temperature at 0.1 wt %; soft gel formation temperature at 1 wt % and hard gel formation temperature at the critical gelation concentration. The cloud points of 1 wt % solutions are in good agreement with the measurements of Bahadur and co-workers.[26] KF and KCl decrease the temperature limit of solubility, and the solvent becomes poorer for P-85 with these salts. KSCN makes the solvent better, giving a higher temperature for the transition to the two-phase region. The sphere-to-rod transition temperature has only been determined for the KF systems in this work, but similar data were obtained for P-85 in pure water by Schillén and co-workers.[20] Table 2 shows that the shift in temperature is largest in 1 M KF with all four transitions. These shifts are approximately twice the shift values observed in 0.5 M KF, indicating a linear relationship with salt concentration. The effects in 1 M KCl are of the same magnitude as in 0.5 M KF.

The observations[25,26] of equivalent properties for polymer solutions with different salt contents at a fixed temperature below the cloud temperature were tested for the four transitions. For the sphere-to-rod transition there is a good agreement for the salt-free system and the two KF systems, all transitions commencing about 13 °C prior to clouding. Reasonably good agreement is seen for the soft gel formation, where in the salt-free system gelation starts at about 5 °C before clouding and in the salt systems between 3 and 9 °C before clouding. The temperatures of formation of the hard gels do not follow the same pattern, however. The hard gel forms at 48 deg below the cloud point in the salt-free system, but 39 deg below in 1 M KF and 55 deg below in KSCN.

Another way of comparing the salt effects is shown in parentheses in Table 2, where the difference between a transition temperature for the salt-free system and the corresponding temperature for the salt-containing system is shown as ΔT ($T_{H_2O} - T_{salt}$). This shows that

the effect of a given salt is fairly constant for the three upper transitions, but deviates for the hard gel formation. The three upper transitions are usually[19,42,43] attributed to changes in PEO-block solvation only. PEO coils are less expanded as water progressively becomes a poorer solvent, with increasing temperature.[11] As the PEO blocks contract with increasing temperature, the solvation capacity for the micelles decreases. To compensate for this, a larger amount of PEO blocks is needed to cover the micellar surface and the spherical micelles increase in size. The upper limit in size for the spherical micelle is given by the PPO blocks,[18] which extend from one side of the micelle to the other. Therefore, the contraction of PEO blocks forces the micelles to change from a spherical to a rod-like shape.[19] With increasing temperature the rod-like micelles grow in length and interact to form a soft gel. Finally, at the cloud point temperature water has become a sufficiently poor solvent for the PEO blocks, and attractive forces between the PEO-blocks cause phase separation.[44] A fairly constant temperature difference (ΔT) for each salt is therefore expected for the three upper transitions. The hard gel formation on the other hand is controlled by both the PPO-block and the PEO-block solvation. To form this gel, the hard sphere volume fraction of the spherical micelles must exceed a critical value of 0.53.[18,21,45] The equilibrium between unimers and micelles is forced toward micelles with increasing temperature due to hydrophobic interactions between the PPO blocks and water. This increases the volume fraction of the spherical micelles. A decrease in volume fraction is induced by contraction of the PEO block with temperature. The temperature dependences of these two opposite functions determine the critical gelation temperature for the hard gel. The onset of micelle formation is also shifted by the salts in the same direction as the cloud points, but by a much smaller amount.[26] This shows a weaker effect of salts on the PPO block than on the PEO blocks, which explains the reduced effect on the hard gel formation temperature.

E. Hard Gel Formation. The critical gelation concentration (cgc) for the salt-free P-85 system is 23.4 wt %.[46] Addition of 1 M KCl hardly changes the cgc, which for this system is 23.3 wt %. Both KF and KSCN have a more pronounced effect on the cgc, which for both salts increases: 1 M KSCN (26.3 wt %); 1 M KF (27.8 wt %); 0.5 M KF (25.5 wt %). The mechanism underlying the elasticity of the hard gel is not well understood, but some parameters show common values for gel formation with a number of PEO/PPO/PEO triblock copolymers. As mentioned above, hard gels are formed when the micellar hard-sphere volume fraction reaches a value of 0.53 and the micelles close-pack in the bcc structure.[18] The concentration of EO in solution is found to be constant at about 15 wt % at the critical gelation concentration for five copolymers (P-84, P-85, F-87, F-88, and P-94).[47] The EO concentration at the cgc can be calculated from the composition of the copolymers with correction for the solution volume occupied by PPO. The solvation properties of the salt-free solvent for the EO blocks in these five copolymers are fairly similar due to a limited temperature difference between the critical gelation temperatures. The salts seem to have a stronger influence on the EO-block solvation. The PEO-block solubility is negatively affected by the addition of KF and KCl. A contraction of these blocks, and therefore an increase in the cgc is expected. This is only seen for the two KF systems and not for the KCl system. There is a positive effect of KSCN on the PEO-block solubility. Extension of these blocks and a decrease in the cgc are therefore expected. The observed effect is opposite, however: the cgc increases by almost 3 wt %. The salt effect on the PPO blocks thus possibly exceeds the expected effect on the EO blocks.

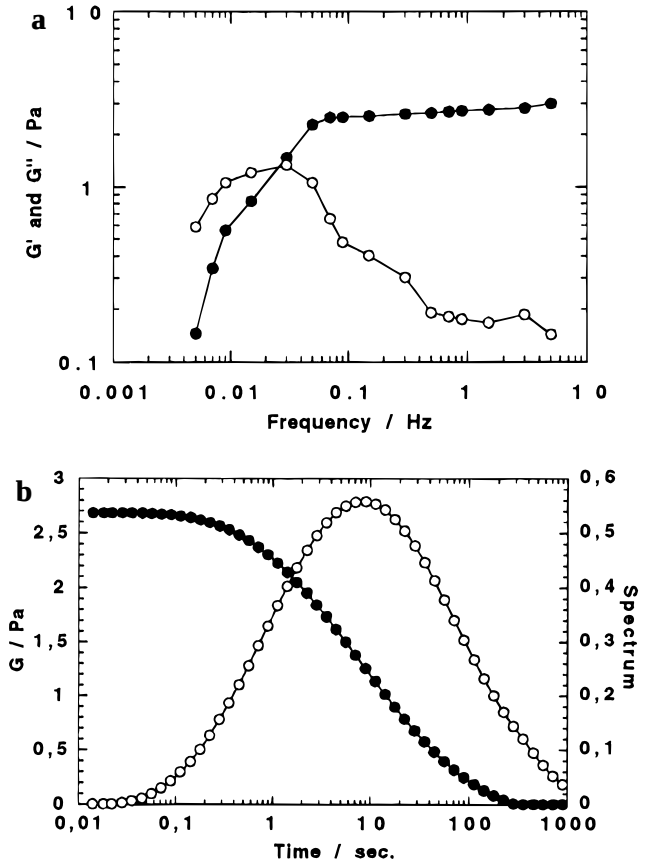

Figure 7. (a) Viscoelastic properties of 3.0 wt % P-85 in 1 M KCl as a function of angular frequency at 65 °C: (●) G' and (○) G''. (b) Stress relaxation for the same sample at 65 °C. (●) is the smoothed relaxation modulus, and (○) is the corresponding relaxation spectrum.

F. Soft Gel. To further investigate the soft gel, the viscoelastic properties were also studied as a function of angular frequency. Figure 7a shows G' and G'' plotted against frequency for a 3.0 wt % P-85 solution in 1 M KCl at 65 °C. At low frequencies G'' is larger than G', which is characteristic for a viscoelastic liquid. At high frequencies the G' values reach a plateau and exceed G''. This characterizes the gel state. At an intermediate frequency G' crosses G'', and the frequency, ν_c, for crossover is characteristic for the sample, giving the relaxation time ($\tau = 1/(2\pi\nu_c)$). Figure 7b shows, for the same sample, stress relaxation measurements. These were performed as another independent way of determining the relaxation time. The figure shows the smoothed stress relaxation modulus against time, and the relaxation spectrum. There is good agreement for all samples between the relaxation time calculated from oscillatory measurements and the dominant relaxation time in the spectrum. The dominant relaxation time for this sample is plotted in Figure 8a together with the relaxation times for other concentrations of P-85 in 1 M KCl at 65 °C. The data show a weak decrease in relaxation time with concentration. For a system of rods the relaxation time is expected to increase with concentration as the rotation becomes

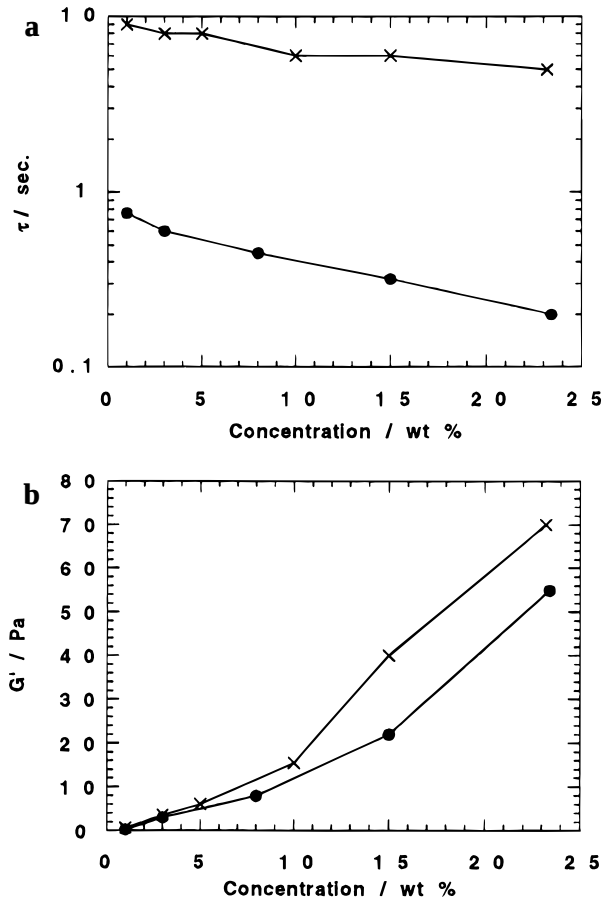

Figure 8. (a) Relaxation times as a function of concentration. (×) is P-85 in 1 M KCl at 65 °C, and (●) is P-85 in water at 80 °C. (b) The G' plateau value as a function of concentration. Symbols as in (a).

more hindered.[40] However, a decrease is seen, also in Figure 8a, for the salt-free P-85 system at 80 °C. The relaxation times are seen to be about 1 order of magnitude faster for the salt-free system, which was analyzed at a temperature 15 °C above the KCl system. The longer relaxation time observed for the KCl system is most likely due to the differences in temperatures and the fact that 1 M KCl is a poorer solvent than water for the unimers. A possible explanation for the relaxation mechanism is the partial breakdown or dissolution of the rod-like micelles. The kinetics in the equilibrium between unimers and micelles, or the exchange rate between micelles, presumably control the time for micellar crossing and thereby the relaxation time. A similar explanation was given by Shikata and co-workers[48,49] for a detergent micellar system with a cosolute.

The decrease in the relaxation time with increasing concentration for the soft gels is not explained by the above presented theory. One possible explanation for this decrease could be an increasing tension in the cross points with increasing concentration. The G' values for the soft gels corresponding to Figure 8a, are shown in Figure 8b. The storage moduli, G', are not linear in c, which the rigid rod theory predicts.[40] Neither is G' linear in c^2, which is predicted by the theory for flexible polymer chains.[30] The observed concentration dependence may indicate partly flexible rods, with increasing cross point tension with concentration, and thereby a reduced relaxation time.

Another example of the remarkable behavior in the relaxation times is seen in Figure 9, where data for 15

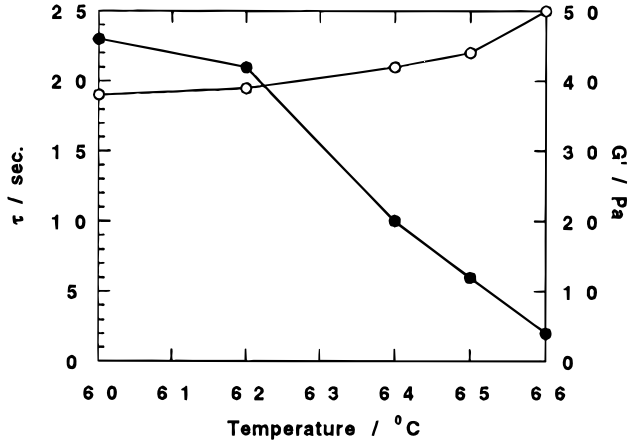

Figure 9. Relaxation time and G'-plateau value against temperature for 15.0 wt % P-85 in 1 M KCl. (●) is relaxation time, and (○) is the modulus.

wt % P-85 in 1 M KCl are plotted against temperature. According to the estimations of rod length, Table 1, the rod length increases with temperature. For rigid rods and flexible chains this should increase the relaxation time. Although the number of micelles decreases when they grow, this effect on the relaxation time should be more than compensated for by the strong length dependence of the relaxation time. The figure shows, as in Figure 8a, a decrease in relaxation times. The decrease in relaxation time is 1 order of magnitude when the temperature is increased from 60 to 66 °C. This cannot be explained by the change in solvent viscosity and diffusion. The theory of partial breakdown or dissolved micelles, however, agrees with these results, since an increased exchange rate is expected with temperature.

The soft gel has different properties at high concentrations, both with and without salt. To examine these differences, the viscoelastic properties were determined as a function of strain amplitude. Figure 10a shows G' and G'' as a function of strain for a 32 wt % P-85 solution without salt at 80 °C and at a frequency of 0.15 Hz. For small deformations the samples exhibit gel-like behavior, since G' is much larger than G''. As the deformation is increased, the modulus of the gel decreases, and at the apparatus limit of deformation, the sample has almost become a viscoelastic liquid. This behavior is concentration-dependent, as seen in Figure 10b, where G' for four concentrations of P-85 at 80 °C is plotted against strain amplitude. Up to around 27 wt %, G' is independent of strain but, as seen for the 27 wt % sample, a strong strain dependence occurs around strain amplitudes of 0.05. For the 32 wt % sample the strain dependence occurs already around 0.01. These changes occur in the concentration range where the P-85 soft gel is observed to crystallize.[20,21] The increase of the G' plateau value is seen to be very strong between 26.4 and 27 wt % where the system starts to order. The very abrupt strain dependence seen for the 27 wt % sample may indicate alignment of the rods by shearing, which also was observed in the salt-free system using a visual flow birefringence test.[20] An increase in the G' plateau value is seen in repeated measurements. This hardening, created by larger deformation, is due to increased order in the structure. The ordered structure is more sensitive to strain, the strong dependence now occurs at strain amplitudes around 0.01, as seen for the 32 wt % sample. At the highest concentration where the ordered structure is established, the relaxation time for

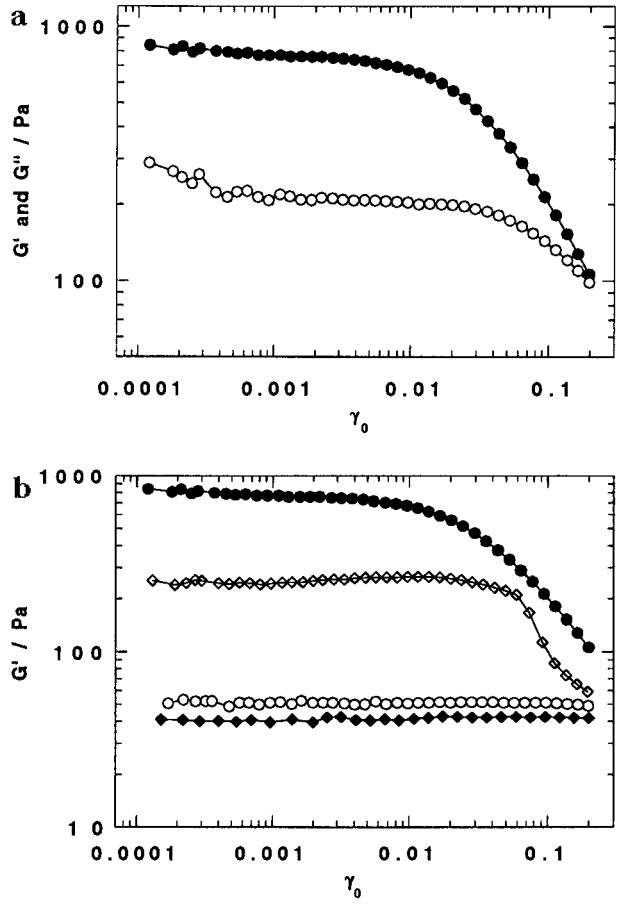

Figure 10. (a) Viscoelastic properties, (●) G' and (○) G'', of 32.0 wt % P-85 in water at 80 °C and 0.15 Hz as a function of strain amplitude. (b) G' for P-85 in water against strain amplitude at 80 °C and 0.15 Hz for solutions with concentrations in wt %: (◆) 23.0; (○) 26.4; (◇) 27.0; (●) 32.0.

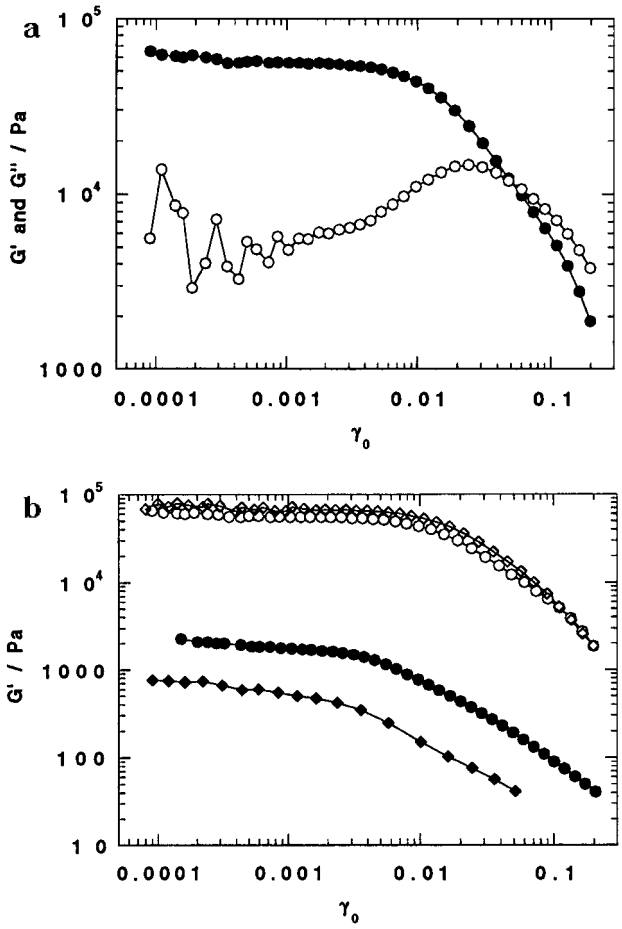

Figure 11. (a) Viscoelastic properties, (●) G' and (○) G'', of 30.0 wt % P-85 in water at 39 °C and 0.15 Hz as a function of strain amplitude. (b) G' for P-85 in water against strain amplitude at 39 °C and 0.15 Hz for solutions with concentrations in wt %: (◆) 23.6; (●) 24.0; (○) 30.0; (◇) 32.0.

the gel lies outside the frequency range for the rheometer (τ > 160 s), but large deformations disrupt the crystal and thereby weaken the gel.

The strain dependence of the soft gel at the highest concentration is similar to the strain-dependent behavior of the hard gel. Figure 11a shows G' and G'' against strain amplitude for a 30 wt % P-85 solution without salt at 39 °C at a frequency of 0.15 Hz. At small deformation, the sample has a gel-like character, but as the deformation is increased, the gel weakens and, already at strain amplitudes around 0.05, G'' exceeds G'. With a further increase in strain, the loss modulus of the viscoelastic liquid decreases. The relaxation time for the hard gel lies outside the frequency range for the rheometer. The influence of concentration on the strain dependence for the hard gel is shown in Figure 11b, where G' for four concentrations of P-85 at 39 °C is plotted against strain amplitude. The gel strength is seen to increase with concentration, both with respect to the G' plateau values and with respect to the deformation dependence. At the highest concentration, G' is constant to larger strain amplitudes, whereas at 23.6 wt %, which is just above the cgc, G' shows a weak strain dependence even at very low strain amplitudes. These strain-dependent properties are shared by all systems with or without salt.

IV. Conclusion

The micellization and gelation of P-85 in salt-containing solutions follow the same pattern as the salt-free system, but temperatures for the micellar sphere-to-rod transition, gel formation, and cloud points are shifted with salt addition. The temperature shifts for rod and soft gel formation are equal to the temperature shifts in the cloudpoints for the different systems. The observed temperature shifts are proportional to the salt concentrations. Estimations of the micellar rod length in the 1 M KF system at 40 °C gave size limits between 1000 and 1800 Å. The decreases in relaxation time with concentration for the soft gels are attributed to partial breakdown of the micellar rods at the cross points. At around 27 wt % in aqueous solution, the rods in the soft gel start to order.

Acknowledgment. This work was supported in part by the Swedish Technical Research Council (TFR) and the Danish Research Academy.

References and Notes

(1) Lundsted, L. G.; Schmolka, I. R. In *Block and Graft Polymerization*; Ceresa, R. J., Ed.; John Wiley & Sons: London, 1976; Vol. 2, pp 1−111.
(2) Almgren, M.; Brown, W.; Hvidt, S. *Colloid Polym. Sci.* **1995**, *273*, 2−15.
(3) Chu, B. *Langmuir* **1995**, *11*, 414−421.
(4) Alexandridis, P.; Hatton, T. A. *Colloid Surf. A* **1995**, *96*, 1−46.
(5) Glatter, O.; Scherf, G.; Schillén, K.; Brown, W. *Macromolecules* **1994**, *27*, 6046−6054.
(6) Brown, W.; Schillén, K.; Hvidt, S. *J. Phys. Chem.* **1992**, *96*, 6038−6044.
(7) Rassing, J.; Attwood, D. *Int. J. Pharm.* **1983**, *13*, 47−55.
(8) Wanka, G.; Hoffmann, H.; Ulbricht, W. *Colloid. Polym. Sci.* **1990**, *268*, 101−117.

(9) Zhou, Z.; Chu, B. *J. Colloid Interface. Sci.* **1988**, *126*, 171−180.
(10) Wanka, G.; Hoffmann, H.; Ulbricht, W. *Macromolecules* **1994**, *27*, 4145−4159.
(11) Hvidt, S.; Jørgensen, E. B.; Schillén, K.; Brown, W. *J. Phys. Chem.* **1994**, *98*, 12320−12328.
(12) Alexandridis, P.; Holzwarth, J. F.; Hatton, T. A. *Macromolecules* **1994**, *27*, 2414−2425.
(13) Schick, M. J. *Nonionic surfactants. Physical chemistry*; Marcel Dekker Inc.: New York, 1987.
(14) Tuzar, Z.; Kratochvíl, P. *Adv. Colloid Interface Sci.* **1976**, *6*, 201−232.
(15) Hvidt, S. *Colloid Surf. A* **1996**, *112*, 201−207.
(16) Fleischer, G. *J. Phys. Chem.* **1993**, *97*, 517−521.
(17) Mortensen, K.; Pedersen, J. S. *Macromolecules* **1993**, *26*, 805−812.
(18) Mortensen, K.; Brown, W. *Macromolecules* **1993**, *26*, 4128−4135.
(19) Linse, P. *J. Phys. Chem.* **1993**, *97*, 13896−13902.
(20) Schillén, K.; Brown, W.; Johnsen, R. M. *Macromolecules* **1994**, *27*, 4825−4832.
(21) Mortensen, K. *Europhys. Lett.* **1992**, *19*, 599−604.
(22) Jørgensen, E. B.; Jensen, J. H.; Hvidt, S. *J. Non-Cryst. Solids* **1994**, *172−174*, 972−977.
(23) Bahadur, P.; Pandya, K. *Langmuir* **1992**, *8*, 2666−2670.
(24) Schott, H.; Royce, A. E.; Han, S. K. *J. Colloid Interface Sci.* **1984**, *98*, 196−201.
(25) Binana-Limbelé, W.; Os, N. M. V.; Rupert, L. A. M.; Zana, R. *J. Colloid Interface Sci.* **1991**, *144*, 458−467.
(26) Bahadur, P.; Pandya, K.; Almgren, M.; Li, P.; Stilbs, P. *Colloid Polym. Sci.* **1993**, *271*, 657−667.
(27) Florin, E.; Kjellander, R.; Eriksson, J. C. *J. Chem. Soc., Faraday Trans. 1* **1984**, *80*, 2889−2910.
(28) Thiyagarajan, P.; Chaiko, D. J.; Hjelm, R. P., Jr. *Macromolecules* **1995**, *28*, 7730−7736.
(29) Reddy, N. K.; Fordham, P. J.; Attwood, D.; Booth, C. *J. Chem. Soc., Faraday Trans.* **1990**, *86*, 1569−1572.
(30) Ferry, J. D. *Viscoelastic Properties of Polymers*, 3rd. ed.; Wiley: New York, 1989.
(31) Nicolai, T.; Brown, W.; Johnsen, R. M.; Stepánek, P. *Macromolecules* **1990**, *23*, 1165−1174.
(32) Pecora, R. *J. Chem. Phys.* **1968**, *48*, 4126−4128.
(33) Flamberg, A.; Pecora, R. *J. Phys. Chem.* **1984**, *88*, 3026−3033.
(34) Broersma, S. *J. Chem. Phys.* **1960**, *32*, 1626−1631.
(35) Broersma, S. *J. Chem. Phys.* **1960**, *32*, 1632−1635.
(36) Broersma, S. *J. Chem. Phys.* **1981**, *74*, 6989−6990.
(37) Zero, K. M.; Pecora, R. *Macromolecules* **1982**, *15*, 87−93.
(38) Brown, W.; Schillén, K.; Almgren, M.; Hvidt, S.; Bahadur, P. *J. Phys. Chem.* **1991**, *95*, 1850−1858.
(39) Schillén, K.; Glatter, O.; Brown, W. *Prog. Colloid Polym. Sci.* **1993**, *93*, 66−71.
(40) Doi, M.; Edwards, S. F. *The Theory of Polymer Dynamics*; Oxford University Press: Oxford, U.K., 1986.
(41) Jørgensen, E. B.; Hvidt, S.; Brown, W. *Annu. Trans. Nordic Rheol. Soc.* **1993**, *1*, 34−36.
(42) Linse, P.; Björling, M. *Macromolecules* **1991**, *24*, 6700−6711.
(43) Kjellander, R.; Florin, E. *J. Chem. Soc., Faraday Trans. 1* **1981**, *77*, 2053−2077.
(44) Karlström, G. *J. Phys. Chem.* **1985**, *89*, 4962−4964.
(45) Mortensen, K.; Brown, W.; Nordén, B. *Phys. Rev. Lett.* **1992**, *68*, 2340−2343.
(46) Glatter, O.; Scherf, G.; Schillén, K. Submitted to *J. Chem. Phys.*
(47) Frederiksen, H.; Hansen, N.-H.; Hornbøll, L.; Jensen, M. T.; Neerup, T. S.; Rasmussen, M. K.; Hvidt, S. *Annu. Trans. Nordic Rheol. Soc.* **1994**, *2*, 97−99.
(48) Shikata, T.; Hirata, H.; Kotaka, T. *Langmuir* **1987**, *3*, 1081−1086.
(49) Shikata, T.; Hirata, H.; Kotaka, T. *Langmuir* **1988**, *4*, 354−359.

MA9616322